Int. J. Environ. Sci. Technol. (2016) 13:733–742
DOI 10.1007/s13762-015-0919-6

ORIGINAL PAPER

Sorption, kinetics and thermodynamics studies of atrazine herbicide removal from water using iron nano-composite material

I. Ali[1] · Z. A. ALOthman[2] · A. Al-Warthan[2]

Received: 12 February 2015 / Revised: 3 November 2015 / Accepted: 7 December 2015 / Published online: 22 December 2015

Abstract Atrazine organic pollutant has been found in several water resources of the world. It is highly toxic and carcinogenic in nature. Atrazine is removed by adsorption on iron composite nanoparticles. The composite nanoparticles were synthesized, analyzed and applied for atrazine uptake from water. Residual atrazine was monitored by gas chromatography–mass spectrometry. The maximum atrazine removal (95 %) was achieved using contact time 30.0 min, concentration 30.0 µg/L, pH 7.0, dose 2.5 g/L and temperature 20.0 °C. The adsorbent was selective for atrazine adsorption. The results obeyed Langmuir, Freundlich, Temkin and Dubinin–Radushkevich isotherms. $\Delta G°$ values were −6.05, −6.11 and −6.15 kJ/mol at 20, 25 and 30 °C temperatures, respectively. The value of $\Delta S°$ was -2.45×10^{-3} kJ/mol K. It showed decline in entropy of atrazine uptake. The adsorption followed pseudo-second-order kinetics. The adsorption mechanism was liquid film diffusion. The proposed adsorption method is inexpensive, fast and reproducible. It can be used to remove atrazine from any water sample/source.

Keywords Adsorption · Atrazine · Gas chromatography–mass spectrometry · Iron composite nanoparticles · Isotherms · Kinetics · Thermodynamics · Water treatment

Introduction

Nowadays, the natural water resources are being contaminated by different pollutants due to over growth of the population and industrialization. There are various types of pollutants at different places, which exist for a long time in the environment (Ali and Aboul-Enein 2004). Atrazine (2-chloro-4-ethylamino-6-isopropylamino-*s*-triazine) is a toxic herbicide, which transports from one place to other. Atrazine is used to manage leafy and grassy weeds in various crops such as pineapples, sugarcane, corn, sorghum, raspberries, roses and juvenile woodland. Besides, it is being used to control landscape vegetation (Dean et al. 1996; Nwani et al. 2010). In spite of the application of atrazine for good crops production, it contaminates the environment through soil and water (Yoder et al. 1973; Stevens and Sumner 1991; Van Leeuwen et al. 1999). Moreover, contamination of atrazine also affects the ecosystem (Yoder et al. 1973; Stevens and Sumner 1991; Van Leeuwen et al. 1999; Nakamura et al. 2000). The bio-accumulation of atrazine into the food chain (animals and human beings) leads to various notorious health hazards and environmental effects. The most serious side effects of atrazine pollution are endocrine disruptor, teratogen, retarding sexual and embryo development, variations in pubertal growth in the living things (Chapin et al. 1996; Munger et al. 1997; Kniewald et al. 2000; Thorpe and Shirmohammadi 2005; Villanueva et al. 2005; Atrazine 2007), non-Hodgkin's lymphoma, etc. (U.S. EPA 2003; U.S. ATSDR 2003).

Atrazine is found in the ground water at several places of the world (Ritter 1990; Southwick et al. 2002; Phyu et al. 2004; Thorpe and Shirmohammadi 2005; Gilliom et al. 2006; Sanagi et al. 2015). The scientists, governments and non-governmental organizations (NGOs) are very much concerned to this herbicide. In view of these facts, it was

✉ I. Ali
drimran_ali@yahoo.com

[1] Department of Chemistry, Jamia Millia Islamia (Central University), New Delhi 110025, India

[2] Department of Chemistry, College of Science, King Saud University, Riyadh 11451, Kingdom of Saudi Arabia

considered worthwhile to develop fast, effective, economic and reproducible method for the subtraction of atrazine from water. The literature shows some adsorption methods for the removal of atrazine (Gai et al. 2011; Zhang et al. 2011; Chaparadza and Hossenlopp 2012; Báez et al. 2013; Silva et al. 2013; Zhao et al. 2013; Yola et al. 2014; Gupta et al. 2015). It was observed that some methods work at extreme pHs, which are not suitable to work under natural water conditions. Besides, it was also found that these methods have high contact times and adsorbent doses. These limitations did not allow these methods to be economic and feasible in the real-world problems. The diverse types sorbents have been reported for the uptake of many contaminants from aqueous solutions (Ali 2010, 2012, 2014; Ali and Gupta 2006; Ali et al. 2012), but nano-adsorbents are ahead of commercial adsorbents for water treatment in this century due to their characteristic features (Ali 2012). The composite nano-materials can be obtained as per the needs. Hence, iron nanoparticles (INPs) were prepared using environment-friendly technology (Huang et al. 2014). The composite INPs were obtained by treating with 1-butyl-3-methylimidazolium bromide. Therefore, the attempts were made to develop fast, economic, environment-friendly and reproducible removal of atrazine using composite INPs. This paper presents the removal of atrazine from water. Atrazine was analyzed by GC–MS, and the findings are discussed herein.

Date and location of the research

The research was conducted on August 1 to November 25, 2014, at Department of Chemistry, Jamia Millia Islamia (Central University), Jamia Nagar, New Delhi 110025, India.

Materials and methods

Chemicals and equipments

Riedel-de-Haen (Seelze, Germany) provided atrazine. Sigma-Aldrich Co., USA, supplied 1-butyl-3-methylimidazolium bromide. HPLC-grade CH_3COCH_3, ACN and MeOH were procured from Merck, Mumbai, India. Millipore-Q, Bedford, MA, USA system was used to prepare deionized water. Gas chromatograph–mass spectrometer (Palo Alto, CA, USA) of Agilent Technology was used for atrazine determination. Gas chromatograph–mass spectrometer has HP Ultra 2 capillary column (25 m × 0.2 mm i.d., and 0.33-μm film thicknesses), mass detector (model 5973) and MSD ChemStation software. The carrier gas was helium. pHs of the solutions were measured using Control Dynamics (APX175 E/C) pH meter. The composite INPs were separated by Remi centrifuge (model C-30BL) machine. Philips PX-1830 diffractometer was used to carry out powdered X-ray diffraction studies. X-ray diffractometer was operated with $\lambda = 1.54$ Å of Cu Kα radiation, secondary optics of Cu filter on, voltage of 25 kV, current of 30 mA with a proportional counter detector.

Synthesis of composite INPs

Green technology was used to prepare iron nanoparticles (NPs) (Hoag et al. 2009; Shahwan et al. 2011). 100.0 g/L Black tea was heated (at 80 °C) for 1 h followed by filtration of the extract. 100 mL of tea extract was mixed with 200 mL 0.20 M ferrous sulfate solution. This solution gave INPs after keeping undisturbed for 24 h. The INPs were centrifuged and separated. INPs were washed with deionized water (three times). Furthermore, these were dried in an oven at 250 °C for 24 h. 2.5 g 1-Butyl-3-methylimidazolium bromide was dissolved in acetate buffer (50 mM, pH 4.5; 100 mL). 5.0 g INPs were taken in a beaker and a solution of 1-butyl-3-methylimidazolium bromide (0.1 L) was added. The beaker was sonicated continuously for 24 h. The impregnated or composite or functionalized INPs were centrifuged for separation and washed with water (three times). Furthermore, the separated INPs were dried in oven (100 °C) for 24 h. The synthesized INPs were used for the removal of atrazine removal.

Characterization of composite nanoparticles

The composite INPs were characterized by UV–Vis spectrometry, XRD and SEM methods. The morphology of INPs was evaluated by field emission scanning electron microscope (FESEM) at various magnifications (10 kV). X-ray diffraction (XRD) studies of untreated and composite INPs were evaluated by X-ray diffractometer (Philips PX-1830) under the experimental conditions as described above. The different angles 10° to 80° 2θ at a scanning rate of 3° 2θ per minute were used to scan functionalized INPs.

Solutions of atrazine

Methanol was used to prepare the standard solution of atrazine (100.0 μg/mL). The solution was put in a freeze of low temperature (−8 °C). The other diluted solutions, for gas chromatograph–mass spectrometer, were prepared in the range of 0.50-80.0 μg/L. On the other hands, these solutions were in the range of 10–50 μg/mL for batch experiments.

Adsorption batch experiments

The adsorption batch studies were done at water bath (thermostatic) with shaking at specific temperature for fixed time. The solid and liquid portions of the experiments were separated by centrifugation. GC–MS was used to monitor equilibrium concentrations of atrazine. The adsorption isotherms of atrazine were carried out at 5–50 µg/L concentrations at pHs 1.0–10.0, contact time 5–50 min, dose 0.5–5.0 g/L and temperatures 20.0–30.0 °C. Thermodynamics and kinetics results were analyzed by different models. The equilibrium atrazine uptake capacity was ascertained by batch studies. The following equation was used for the purpose.

$$C_e = (C_i - C_t)/m \tag{1}$$

where C_i, C_t and C_e are initial, at a particular time (t) and equilibrium amounts (µg/L) of atrazine, respectively. m is weight of INPs (g/L). Atrazine removal in percent was determined using Eq. 2.

$$\%\ \mathrm{Removal} = [(C_i - C_t)/C_0] \times 100 \tag{2}$$

where C_i = initial conc. and C_t = conc. at specific time.

Kinetics study of batch experiments

The kinetics studies were carried out by analyzing sorption of atrazine at diverse time intervals. The various concentrations of atrazine were shaken with a fixed amount of composite INPs. The remaining amount of atrazine was monitored by gas chromatograph–mass spectrometer. The adsorption batch studies were completed to match adsorption capacities at various time periods. 100-mL capacity Erlenmeyer's flasks containing fixed and exact concentrations of atrazine were shaken on a thermostatic water-bath shaker. The fixed concentrations of the composite INPs were added to different containers with continuous trembling. Later on, the INPs were separated and solutions were used for the analysis of atrazine. The experimental errors were ascertained by blank experiments under the similar experimental conditions.

Gas chromatograph–mass spectrometer determination

Qualitative and quantitative measurements of atrazine were completed using GC–MS instrument as discussed above. Atrazine solution (2.0 µL of 100.0 µg/mL) was loaded onto GC–MS machine in split mode. 1.0 mL/min flow rate of helium gas was maintained in GC–MS. Initially temperature was 150 °C with a raise of 5 °C/min to 200 °C. Temperature of GC–MS oven and injection point was adjusted to 250 °C.

Results and discussion

Characterization of composite nanoparticles

Synthesis of INPs was ascertained by monitoring alterations in the peak areas of caffeine (275 nm) and polyphenols (205 nm) present in tea solution. This was realized that areas of the peaks are departed by adding the solution of $FeSO_4$. It established the synthesis of iron NPs. It was concluded that caffeine/polyphenols of tea extract formed INPs owing to their capping and reducing features (Hoag et al. 2009; Shahwan et al. 2011; Huang et al. 2014). The INPs images taken by FESEM were indicative of spherical shape having 40–50 nm diameter (Fig. 1). XRD spectra showed two peaks at 25° θ of FeOOH [iron(III) oxide–hydroxide] and at 29° θ of Fe_2O_3 (maghemite) (Fig. 2). This was remarkable to observe that the peaks vanished after the impregnation of INPs with 1-butyl-3-methylimidazolium bromide. This was owing to 1-butyl-3-methylimidazolium chloride reaction with INPs. This was indicative of the preparation of functionalized INPs.

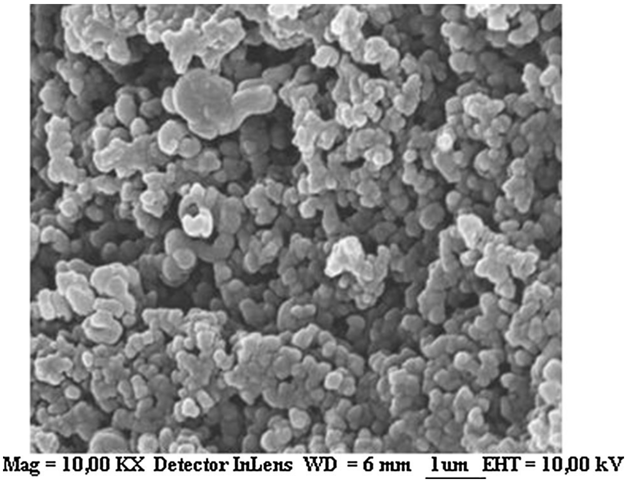

Fig. 1 FESEM image of iron composite nanoparticles

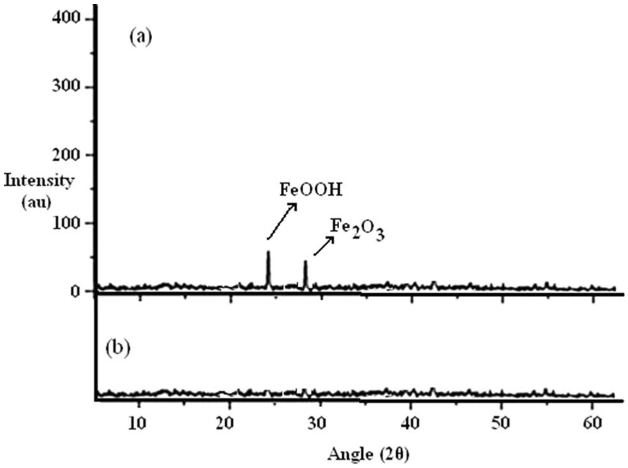

Fig. 2 XRD patterns of (*a*) native and (*b*) iron composite nanoparticles

GC–MS analyses

GC–MS analyses resulted into base line separation of atrazine with a retention time of 7.40 min. Peak of atrazine was confirmed by chromatogram of its standard under similar experimental conditions. The optimization was carried out by changing temperatures of injector and column and flow rate of helium carrier gas. Additionally, MS detector was optimized to obtain the minimum detection limit. Besides, loaded amount of atrazine was also optimized. After exhaustive experiments, the best GC–MS conditions were developed and used. Linearity was observed in the range of 0.10 to 50 μg/L and used for the calibration curve. The coefficient of determination (r^2) was 0.999. LOD determined by the standard method (Watson 1999) was 0.4 μg/L.

Concentration effect

The effect of concentration is very important in adsorption study, which was optimized using 5.0–50.0 μg/L concentrations of atrazine. The remaining experimental parameters were 30-min contact time, 2.5 g/L dose, 7.0 pH and 20 °C temperature. The results of concentration parameter are plotted in Fig. 3a. This figure shows highest atrazine removal at 30.0 μg/L. Initially, adsorption augmented quickly in the range of 5.0–30.0 μg/L concentrations of atrazine. The amounts of atrazine adsorbed were 2.0, 4.0, 7.80 and 11.4 μg/g at 5.0, 10.0, 20.0 and 30.0 μg/L concentrations, respectively. Furthermore, raise of atrazine concentrations to 50 μg/L could not result in more adsorption. Hence, 30.0 μg/L of atrazine was considered as the optimized concentration. The percent removal of atrazine at this concentration was 95.0.

Contact time effect

The contact time was also optimized using 5.0- to 50.0-min experimental times. The other experimental parameters fixed were 30 μg/L atrazine, dose 2.5 g/L, pH 7.0 and temperature 20 °C. The findings of this optimization are plotted in Fig. 3b. This figure depicts that the sorption intensities were 2.0, 4.0, 6.0, 8.0, 9.6 and 11.4 μg/g at 5-, 10-, 15-, 20-, 25- and 30-min contact times, respectively. Furthermore, no raise in adsorption was observed by augmenting contact time. Hence, 30.0 min was considered as the optimum adsorption time. Maximum percentage removal at this experimental time was 95.0.

pH effect

pH is an important parameter to be optimized for maxim removal of pollutants. For this purpose, pHs were ranged from 1.0 to 10.0. The other operating variables were 30 μg/L concentrations of atrazine, 7.0 pH, 2.5 g/L dose and 20 °C temperature. The findings of pH effect are graphed in Fig. 3c. A critical analysis of this figure depicts the adsorption capacities 2, 4, 5.5, 7, 8, 9.5 and 11.4 μg/g at 1, 2, 3, 4, 5, 6 and 7 pHs, respectively. No more adsorption could be observed by further increase in the pHs. Therefore, pH 7.0 was considered as the best one, with the maximum 95.0 % adsorption.

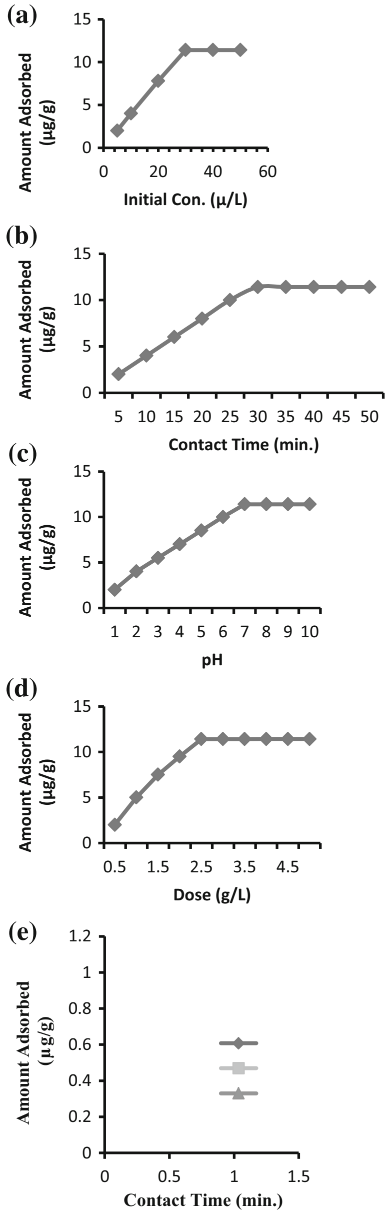

Fig. 3 Optimization of adsorption parameters of atrazine herbicide: **a** initial conc., **b** contact time, **c** pH, **d** dose and **e** temperature

Dosage effect

The economy of the method depends on the dose of adsorption process. Therefore, the doses were varied from 0.5 to 5 g/L. The other experimental conditions were 30.0-min contact time, pH 7.0, 30 μg/L concentrations of atrazine and 20 °C temperature. These findings are plotted in Fig. 3d, which clearly shows sorption capacities of 2, 5, 7.5, 9.5 and 11.4 μg/g at 0.5, 1, 1.5, 2 and 2.5 g/L doses, respectively. Additional dose augment could not give more adsorption. Hence, 2.5 g/L was chosen as the best dose. The percentage removal at this dose was 95.

Temperature effect

Temperature effect on uptake of atrazine was carried out at 20.0, 25.0 and 30.0 °C. The other variables used were 7.0 pH, 30 μg/L concentrations of atrazine, dose 2.5 g/L and 30-min contact time. The outcomes of this study are graphed in Fig. 3e. It was observed that atrazine sorption was decreased with rising temperature. This observation showed adsorption process to be exothermic in nature. Therefore, atrazine sorption was in $20 > 25 > 30$ °C order. These results indicated eco-friendly sorption of atrazine removal, due to temperature range of 20–30 °C of many water resources.

Interfering ions effect

The optimization of adsorption parameters was conducted in Millipore water. The intention of this article is to apply in the real-life problems. Therefore, groundwater containing different ions (sodium, potassium, calcium, magnesium, nitrate, sulfate, chloride, phosphate, etc.) was used to study the ionic interference in atrazine adsorption. For this purpose, the experimentation was also conducted in the groundwater (laboratory tap water). The quality of tap water was ascertained before atrazine adsorption study. pH and conductivity of tap water were measured as 7.19 and 1.48 mS/cm, respectively. The various water quality parameters were hardness (total, 448.0 mg/L), total dissolved solids (TDS, 542.25 mg/L), alkalinity, (280.0 mg/L), potassium (1.84 mg/L), sodium (2.15 mg/L), calcium (204.0 mg/L) and magnesium (244.0 mg/L). The results indicated that 0.8–2 % adsorption decreased in atrazine removal due to the interference of ions present in water. This adsorption decrease may be because of the competitive adsorption among atrazine and interfering ions.

Adsorption isotherms

The results of atrazine uptake were treated by Langmuir, Freundlich and Temkin isotherms. The batch studies were conducted at different temperatures, i.e., 20, 25 and 30 °C, respectively. The outcomes of all three isotherms are discussed in the following subsections.

Langmuir model

Langmuir model explains relationship between adsorbed species and number of active sites of the adsorbent. As per this model, adsorbate is uptaken at a fixed number of definite sites. No further adsorption is possible after the equilibrium of adsorption. All the sites are energetically alike without any interface between contaminate molecules. Langmuir model is applicable for monolayer uptake on a uniform surface. Langmuir adsorption model is shown by Eq. 3.

$$1/Q_t = 1/X_m \cdot b \cdot C_t + 1/X_m \tag{3}$$

where C_t and Q_t are concentration and amount adsorbed of atrazine at time t, respectively. b (L/μg) and X_m (μg/g) are binding energy of atrazine onto the sites of adsorbent and Langmuir constants, respectively (related to the maximum monolayer adsorption capacity of the adsorbent). The values of X_m and b are approximates of the active sites and driving force at equilibrium. These values were calculated from the slope and intercept of plot of $1/Q_t$ versus $1/C_t$. Langmuir graphs for atrazine uptake (at 20, 25 and 30 °C temperature) are plotted in Fig. 4a. The uptake of this herbicide was followed Langmuir isotherm at these temperatures. The regression coefficients (R^2) were 0.578, 0.626 and 0.700 at 20, 25 and 30 °C, respectively. The values of b were 3.73, 2.50 and 1.69 L/μg at 20.0, 25.0 and 30.0 °C, respectively (Table 1), showing a good uptake of herbicide at the reported temperatures. The X_m values were 12.20, 11.76 and 11.36 μg/g at all the reported temperatures. Dimensionless constants (R_L) at the reported temperatures were calculated by Eq. 4.

$$R_L = 1/(1 + b \times C_e) \tag{4}$$

The values of this constant were 0.152, 0.138 and 0.169 at 20, 25 and 30 °C, respectively. Lower than 1.0 value showed favorable adsorption. Table 1 shows that value of R_L was lowest at 20 °C, indicating more favorable adsorption at low temperature.

Freundlich model

Freundlich model applies to both mono- and multilayers adsorption. It also works for both homo- and heterogeneous surfaces. The adsorbate concentration on the surface of INPs is the summation of all the sites. The uptake energies are reduced exponentially on conclusion of adsorption process. Freundlich isotherm is expressed by Eq. 5.

$$\log Q_t = (1/n)\log C_t + \log k_F \tag{5}$$

where k_F [(μg/g)] and n are Freundlich's coefficients corresponding to the relative uptake capacities of INPs and the adsorption intensities. The favorable adsorption occurs if the values of n varied from 1 to 10. Intercept and slope of graph of log Q_t versus log C_t correspond to k_F and $1/n$, respectively. Freundlich's graphs for atrazine adsorption are shown in Fig. 4b with constants values in Table 1. n values at 20, 25 and 30 °C were 12.20, 10.42 and 10.10, respectively, showing favorable adsorption and k_F values were 6.73, 6.40 and

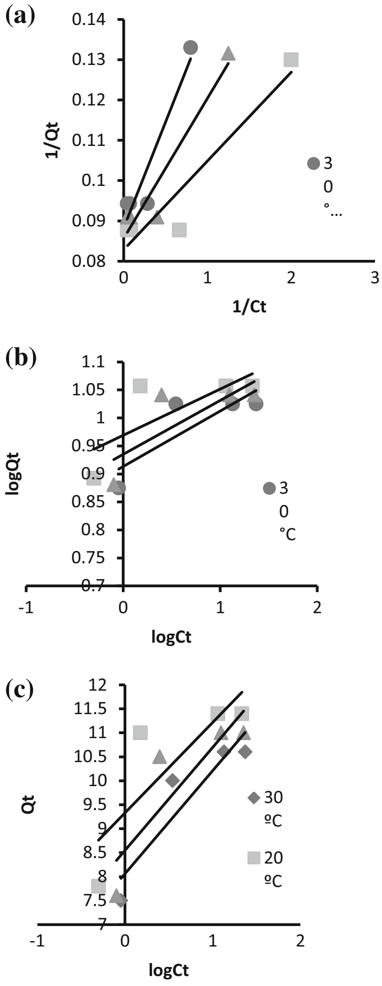

Fig. 4 Plots showing **a** Langmuir, **b** Freundlich and **c** Temkin isotherms for the removal of atrazine herbicide

6.07 μg/g, respectively, showing poor adsorption at high temperature. The regression coefficients were also indicated the most excellent fitting of Freundlich model.

Temkin model

Temkin model is used to explain the adsorbate and adsorbent interactions. Temkin model considers linearly decrease in adsorption heat for all molecules (with surface coverage) owing to adsorbate and adsorbate relations. The uptake is also monitored by a uniform sharing of binding energies. The equation for this model is expressed by Eq. 6.

$$Q_t = (RT/B_T)\ln C_t + (RT/B_T)\ln K_T \tag{6}$$

where K_T (L/g) and B_T (kJ/mol) are related to maximum binding energy and heat of adsorption. T and R are temperature (in Kelvin) and ideal gas constant (0.008314 kJ/mol/K), respectively. The graphs of Q_t versus log C_t of atrazine at all temperature are shown in Fig. 4c. The values of the constants K_T and B_T were designed from the intercept and the slope (Table 1). $B_{T\text{s}}$ were 1.29, 1.15 and 1.10, showing small disparity in the heat of uptake. $K_{T\text{s}}$ were 139.86, 52.88 and 33.83 L/g at three temperatures (20, 25 and 30 °C), indicating strong exchanges between adsorbate and INPs. The regression coefficient (R^2) values showed that the adsorption data followed Temkin model.

Thermodynamic study

Thermodynamics was ascertained by determining free energy change (ΔG^0), enthalpy change (ΔH^0) and entropy change (ΔS^0). The change in ΔG^0 is related to equilibrium constant by Van't Hoffs equation as follows

$$\Delta G^0 = -RT \cdot \ln K \tag{7}$$

where ΔG^0 and T are change in ΔG (kJ/mol) and temperature (K), respectively. R is universal gas constant (0.008314 kJ mol^{-1} K^{-1}), while K is equilibrium constant. On substituting K by Q, the above equation becomes as follows.

$$\Delta G^0 = -RT \times \ln Q^\circ \tag{8}$$

where ΔG^0 values at 20, 25 and 30 °C were −6.05, −6.11 and −6.15 kJ mol^{-1}, respectively (Table 2). Negative values of ΔG^0 supported favorable and spontaneous adsorption. ΔG^0 (Gibbs free energy) is related to changes in ΔS^0 and ΔH^0 as given by Eqs. 9 and 10.

$$\Delta G^0 = \Delta H^0 - T\Delta S^0 \tag{9}$$

$$\ln Q^\text{o} = \Delta S^0/R - \Delta H^0/R \times T \tag{10}$$

Plot of ln Q° versus 1/T was an instant line (diagram is not shown). The intercept and slop corresponded to ΔH^0 and ΔS^0, respectively. The values of ΔH^0 and ΔS^0 were −6.68 and -2.45×10^{-3}. The negative value of ΔH^0 showed exothermic uptake. Small minus value of ΔS^0 was indicative of low entropy of adsorption process. Hence, this was

Table 1 Isotherm parameters values for atrazine

Temps. (°C)	Langmuir isotherm				Freundlich isotherm			Temkin isotherm		
	X_m (μg/g)	b (L/μg)	R_L	R^2	k_F (μg/g)	n (g/L)	R^2	K_T (L/g)	B_T (kJ/mol)	R^2
20	12.20	3.73	0.152	0.903	6.73	12.20	0.578	139.86	1.29	0.680
25	11.76	2.50	0.138	0.918	6.40	10.42	0.626	52.88	1.15	0.754
30	11.36	1.69	0.169	0.904	6.07	10.10	0.700	33.83	1.10	0.849

Table 2 Thermodynamic parameters values for atrazine

$\Delta G°$ (kJ/mol)			$\Delta H°$ (kJ/mol)	$\Delta S°$ (kJ/mol K)
$T = 293$ K	$T = 298$ K	$T = 303$ K		
−6.05	−6.11	−6.15	−6.68	-2.45×10^{-3}

Table 3 Kinetic parameters for atrazine adsorption

Kinetic models	Kinetic parameters	Numerical values
Pseudo-first-order kinetic model	k_1 (min^{-1})	0.069
	Experimental qe (μg/g)	11.40
	Theoretical qe (μg/g)	14.13
	R^2	0.989
Pseudo-second-order kinetic model	k_2 (gμg^{-1} min^{-1})	3.79×10^{-3}
	Experimental qe (μg/g)	11.40
	Theoretical qe (μg/g)	15.87
	h (μgg^{-1} min^{-1})	0.95
	R^2	0.924
Elovich kinetic model	α (μgg^{-1} min^{-1})	15.09
	β (gμg^{-1})	0.22
	R^2	0.887
Intra-particle diffusion kinetic model	k_{ipd1} (μgg^{-1} min$^{-0.5}$)	2.84
	Intercept	4.72
	R^2	0.985
Film diffusion kinetic model	k_{fd} (gμg^{-1})	0.063
	Intercept	0.062
	R^2	0.944

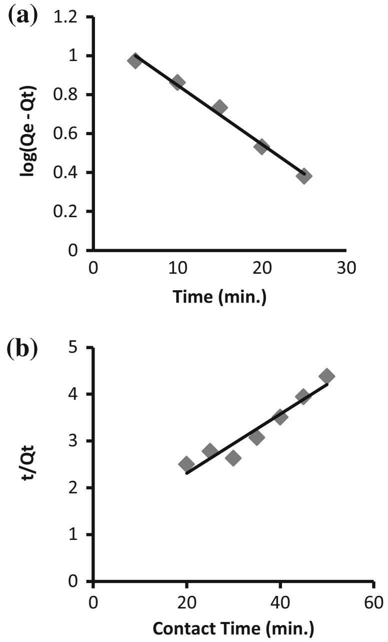

Fig. 5 Plots showing **a** pseudo-first-order kinetic plot and **b** pseudo-second-order kinetic plot

considered that uptake of this herbicide was related to beg off in mobility freedom of the reported pollutant.

Kinetics modeling

Kinetics modeling is used to determine adsorption mechanism. It depends on the physicochemical features of the adsorbate and adsorbent. Therefore, the different kinetic models were used to explain the adsorption findings. These are explained as follows.

Pseudo-first-order kinetic model

First of all, pseudo-first-order kinetic model was used to the experimental findings. It is expressed by Eq. 11.

$$dQ_t/dt = k_1(Q_e - Q_t) \tag{11}$$

On integration of Eq. 11 (with boundary conditions of $t = 0$ with $Q_t = 0$ and $t = t$ with $Q_t = Q_t$), it becomes Eq. 12.

$$\log(Q_e - Q_t) = \log Q_e - k_1 t/2.303 \tag{12}$$

where Q_e and Q_t are atrazine concns. (μg/g) uptaken at equilibrium and time t, respectively. k_1 (min^{-1}) corresponds to equilibrium coefficient of pseudo-first-order uptake. The values are reported in Table 3. k_1 (min^{-1}) was calculated from slop of log ($Q_e - Q_t$) versus t graph (Fig. 5a) at 20 °C temperature. Pseudo-first-order rate coefficient and regression coefficient (R^2) were 0.069 and 0.989 min^{-1}, respectively, showing the applicability of this model. The theoretical and experimental Q_e values were 15.13 and 11.40 μgg^{-1}, respectively, showing 22.7 % higher theoretical value. Therefore, pseudo-first-order kinetic model could not be used exactly. These types of variations are available in the literature (Ho and McKay 1998; Bhattacharyya and Sharma 2005). Therefore, the efforts have also been arranged to test experimental values by pseudo-second-order model.

Pseudo-second-order kinetic model

This model is responsible to explain chemical or exchange uptake. This kinetic model for uptake of pollutant is given by Eq. 13.

$$dQ_t/dt = k_2(Q_e - Q_t)^2 \tag{13}$$

where Q_t, Q_e and t are already described above. This equation was integrated (with boundary conditions of $t = 0$ with $Q_t = 0$ and $t = t$ with $Q_t = Q_t$), resulting into Eq. 14.

$$t/Q_t = 1/k_2 Qe^2 + t/Q_t \tag{14}$$

In Eq. 14, $k_2 Q_e^2$ was substituted by h. It results in the following equation.

$$t/Q_t = 1/h + t/Q_e \tag{15}$$

where h is initial uptake rate coefficient. It can be calculated from pseudo-second-order figure. Q_t/t approached h with reduced time (zero). On the other hand, k_2 is rate coefficient of pseudo-second-order uptake (g/µg/min). Plot of t/Q_t versus t was graphed (Fig. 5b). k_2 and Q_e were calculated from intercept and slope of the graph, respectively (Table 3). The value of k_2 was 3.79×10^{-3} $\text{g}\mu\text{g}^{-1}$ min^{-1}. It was very small in comparison with initial rate coefficient ($h = 1.28$ $\text{g}\mu\text{g}^{-1}$ min^{-1}). Therefore, there was fast speed of adsorption in starting with slow one at boost up of time. Regression coefficient high value ($R^2 = 0.924$) showed applicability of pseudo-second-order model to the uptake data. Besides, experimental and theoretical values of Q_e were quite closer. This observation confirmed the applicability of this kinetic model.

Elovich's model

The adsorption and desorption processes determine the feasibility of the method to solve real-life problems. These can be determined by Elovich's kinetic model, i.e., determination of adsorption and desorption rates (Chien and Clayton 1980). Elovich's kinetic model is expressed by Eq. 16.

$$\mathrm{d}Q_t/\mathrm{d}t = \alpha \exp(-\beta \cdot Q_t) \tag{16}$$

where α (µg/g/min) corresponds to initial adsorption rate with β (g/µg) as desorption rate. Equation 16 was integrated (boundary conditions of $t = 0$ with $Q_t = 0$ and $t = t$ with $Q_t = Q_t$). Furthermore, by presumption of $\alpha \cdot \beta_t \gg 1$, above equation changed to 17.

$$Q_t = 1/\beta \ln(\alpha \cdot \beta) + 1/\beta \cdot \ln t \tag{17}$$

where α, β and R^2 values were 15.09 $\mu\text{g}\text{g}^{-1}$ min^{-1}, 0.22 $\text{g}\mu\text{g}^{-1}$ and 0.887, respectively (Table 3). These values suggested higher rate of adsorption than desorption. The values of α and β were supported fast uptake in the beginning, which became slow with increase in time. Besides, regression constant value was near to one; showing the utility of Elovich's model.

Mechanism of uptake

The film, pore and intra-particle diffusion are the well-known models to determine adsorption process. The sorption process is restricted by the slowest step involved in adsorption phenomenon. The experimental data were fitted to these models. These are discussed below.

Intra-particle diffusion kinetic model

The uptake of atrazine occurred by transport from solution to adsorbent surface, uptake by adsorbent and carries over within the pores of adsorbent. Hence, uptake is controlled either by surface sorption kinetics or carry over process (intra-particle and film diffusions) or by both progressions. Second step is very speedy and cannot be rate fixing. First and third steps may be rate controlling. Hence, these steps were ascertained by two models. Transport of the reported herbicide from solution to INPs sites was considered by the association between atrazine amount up taken and the square root of contact time. The following equation was used for this point.

$$Q_t = k_{\text{ipd}} t^{05} \tag{18}$$

A straight line figure of Q_t versus $t^{0.5}$ (fleeting through the origin) and slope of the line matching to rate constant (k_{ipd}) established uptake as restricted by intra-particle diffusion. This sort of figure was plotted (not given in this paper). Value of rate constant was 2.84 $\mu\text{g}\text{g}^{-1}$ $\text{min}^{-0.5}$. The regression coefficient and intercept values were 4.72 and 0.985, respectively (Table 3). Graph line did not go via the origin. It showed non-applicability of intra-particle diffusion model.

Liquid Film Diffusion Kinetic Model

This model was proposed by Boyd et al. (1947). Boundary acts as a crucial role in uptake process. This model is given by Eq. 19.

$$\ln(1 - Q_t/Q_e) = -k_{\text{fd}} \cdot t \tag{19}$$

Or

$$\ln(1 - F) = -k_{\text{fd}} \times t \tag{20}$$

where k_{fd} is a film diffusion rate coefficient. F (Q_t/Q_e) corresponds to fractional achievement of equilibrium. A plot of ln (1 − F) versus t straight line (with zero intercept uptake process) is preceded by film diffusion means. The values of k_{fd} and intercept were 0.063 $\text{g}\mu\text{g}^{-1}$ and 0.062, respectively (Table 3). A direct line passed through the origin with small deviation of from zero intercept (−0.062). The departure from zero might be because of high agitation velocity in kinetics experimentations. Besides, the disparity between rates of mass transport in early and final stages of uptake might be accountable for small exodus from zero value. There are some papers in the scientific research literature describing the similar results (Cheung et al. 2001; Onyango et al. 2003; Goswami and Ghosh 2005). In view of these facts, uptake of the reported herbicide on composite INPs was restricted by liquid film diffusion mechanism.

Supra-molecular level mechanism

Obviously, nanoparticles are gaining good importance in adsorption of various pollutants from water. Furthermore, the developed iron composite nanoparticles have positive charges. Consequently, this adsorbent shows good

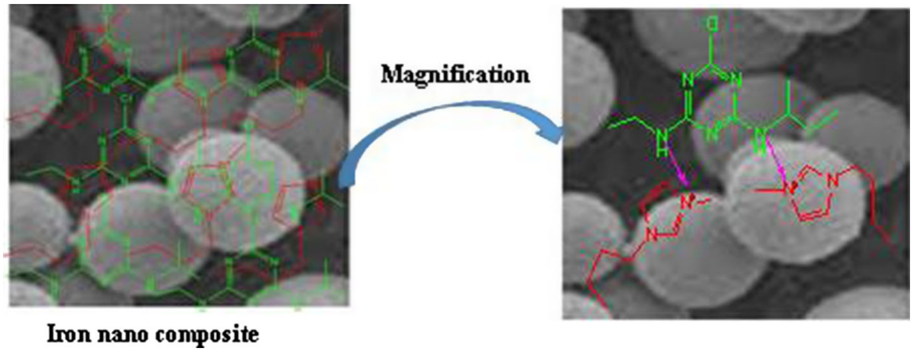

Fig. 6 Mechanism of atrazine herbicide adsorption

attractive forces to seize the reported herbicide on composite INPs. The diagrammatic illustration of the reported herbicide (atrazine) subtraction by sorption is graphed in Fig. 6. This is clear from Fig. 6 that the composite INPs have positive charges. Therefore, lone pairs on nitrogen (of atrazine herbicide) coordinated to the positive charges of the adsorbent. Hence, the molecules of the reported herbicide formed coordination bonds with composite INPs. In this way, the uptake of atrazine herbicide on composite INPs was restricted by chemical bondings. Henceforth, the removal of atrazine herbicide is fast.

Desorption studies

Easy desorption features of the adsorbents make them economic and feasible at practical levels. The regeneration of adsorbent is an important issue in water treatment. Hence, the efforts were made to regenerate adsorbent and recycling. Various acids such as hydrochloric, nitric and sulfuric acids were tried for the purpose. After exhaustive experimentation, the maximum regeneration was obtained by hydrochloric acid. The highest desorption (99 %) was achieved successfully using hydrochloric acid of 100 mN strength. The regenerated composite INPs were applied for seven cycles for uptake of atrazine, with 90–98 % removal capacities.

Applicability of composite INPs in real water samples

The importance of this method was assessed by its applicability for removing the reported herbicide from our water resources. Consequently, this sorption method was used for the removal of atrazine from river water. Ten water samples were collected from diverse location of the Hindon River (India). Atrazine concentrations in different samples were ranged from 0.5 to 18.0 μg/L. The developed composite INPs adsorption method was used to eliminate atrazine from river water. It was found that % removal of this herbicide ranged from 90 to 100. These results obviously indicated that developed sorption method was appropriate for the elimination of atrazine herbicide from ordinary river waters.

Conclusion

The above-discussed results showed that the prepared iron composite nanoparticles was able to remove atrazine herbicide from water successfully up to 95 %. The uptake method was effective and choosy for the removal of atrazine. The removal order of atrazine from water was 20 > 25 > 30 °C, indicating exothermic nature of adsorption. Besides, thermodynamic experiments also confirmed exothermic uptake. Gas chromatograph–mass spectrometric method detected atrazine at minimum level with a detection limit of 0.4 μg/L. The sorption data obeyed Temkin, Freundlich and Langmuir models. Kinetics modeling inveterated pseudo-second-order and liquid film diffusion mechanisms. In a nut shell, the reported sorption method was speedy, economic and environmental friendly because of working capabilities in natural water resources pHs along with low-dose and contact time regimens. Small contact time can be exploited to transfer batch conditions to column operation successfully. Therefore, the presented sorption method may be practical for the removal of the reported herbicide from several water bodies at vast and cost-effective scale.

Acknowledgments The authors are thankful to King Saud University, Riyadh, Saudi Arabia, for Visiting Professor Program.

Compliance with ethical standards

Ethical statement There is no ethical issue related to this manuscript.

References

Ali I (2010) The quest for active carbon adsorbent substitutes: inexpensive adsorbents for toxic metal ions removal from wastewater. Sep Purif Rev 39:95–171

Ali I (2012) New generation adsorbents for water treatment. Chem Rev (ACS) 112:5073–5091

Ali I (2014) Water treatment by adsorption columns: evaluation at ground level. Sep Purif Rev 43:175–2015

Ali I, Aboul-Enein HY (2004) Chiral pollutants: distribution, toxicity and analysis by chromatography and capillary electrophoresis. Wiley, Chichester

Ali I, Gupta VK (2006) Advances in water treatment by adsorption technology. Nat Lond 1:2661–2667

Ali I, Asim M, Khan TA (2012) Low cost adsorbents for removal of organic pollutants from wastewater. J Environ Manage 113:170–183

Atrazine (2007) Chemical Summary, Toxicity and Exposure Assessment for Children's Health Report. U.S. Environmental Protection Agency, USA

Báez ME, Fuentes E, Espinoza J (2013) Characterization of the atrazine sorption process on andisol and ultisol volcanic ash-derived soils: kinetic parameters and the contribution of humic fractions. J Agric Food Chem 61:6150–6160

Bhattacharyya KG, Sharma A (2005) Kinetics and thermodynamics of methylene blue adsorption on neem leaf powder. Dyes Pigm 65:51–59

Boyd GE, Adamson AW, Myers LS (1947) The exchange adsorption of ions from aqueous solutions by organic zeolites. II: Kinetics. J Am Chem Soc 69:2836–2848

Chaparadza A, Hossenlopp JM (2012) Adsorption kinetics, isotherms and thermodynamics of atrazine removal using a banana peel based sorbent. Water Sci Technol 65:940–947

Chapin RE, Stevens JT, Hughes CL, Kelce WR, Hess RA, Daston GP (1996) Endocrine modulation of reproduction. Fundam Appl Toxicol 29:1–17

Cheung CW, Porter JF, McKay G (2001) Sorption kinetic analysis for the removal of cadmium ions from effluents using bone char. Water Res 35:605–612

Chien SH, Clayton WR (1980) Application of Elovich equation to the kinetics of phosphate release and sorption in soils. Soil Sci Soc Am J 44:265–268

Dean JR, Wade G, Barnabas IJ (1996) Determination of triazine herbicides in environmental samples. J Chromatogr A 733:295–335

Gai K, Shi B, Yan X, Wang D (2011) Effect of dispersion on adsorption of atrazine by aqueous suspensions of fullerenes. Environ Sci Technol 45:5959–5965

Gilliom RJ, Barbash JE, Crawford CG, Hamilton PA, Martin JD, Nakagaki N, Nowell LH, Scott JC, Stackelberg PE, Thelin GP, Wolock DM (2006) US Geological Survey, The Quality of Our Nation's Waters: Pesticides in the Nation's Streams and Ground Water, 1992–2001, February 15

Goswami S, Ghosh UC (2005) Studies on adsorption behavior of Cr(VI) onto synthetic hydrous stannic oxide. Water SA 31:57–602

Gupta VK, Yola ML, Eren T, Atar N (2015) Selective QCM sensor based on atrazine imprinted polymer: its application to wastewater sample. Sensors Actuators B: Chem 218:215–221

Ho YS, McKay G (1998) The kinetics of sorption of basic dyes from aqueous solution by sphagnum moss peat. Can J Chem Eng 76:822–827

Hoag GE, Collins JB, Holcomb JL, Hoag JR, Nadagouda MN, Varma RS (2009) Degradation of bromothymol blue by 'greener' nano-scale zerovalent iron synthesized using tea polyphenols. J Mater Chem 19:8671–8677

Huang L, Weng X, Chen Z, Megharaj M, Naidu R (2014) Green synthesis of iron nanoparticles by various tea extracts: comparative study of the reactivity. Spectrochim Acta Part A Mol Biomol Spectrosc 130:295–301

Kniewald J, Jakominić M, Tomljenović A, Simić B, Romać P, Vranesić D, Kniewald Z (2000) Disorders of male rat reproductive tract under the influence of atrazine. J Appl Toxicol 20:61–68

Munger R, Isacson P, Hu S, Burns T, Hanson J, Lynch CF, Cherryholmes K, Van Dorpe P, Hausler WJ Jr (1997) Intrauterine growth retardation in Iowa communities with herbicide contaminated drinking water supplies. Environ Health Perspect 105:308–314

Nakamura C, Hasegawa M, Shimada K, Shirai M, Miyake J (2000) Direct triazine herbicide detection using a self-assembled photosynthetic reaction center from purple bacterium. Biotechnol Bioprocess Eng 5:413–417

Nwani CD, Lakra WS, Nagpure NS, Kumar R, Kushwaha B, Srivastava SK (2010) Toxicity of the herbicide atrazine: effects on lipid peroxidation and activities of antioxidant enzymes in the freshwater fish Channa Punctatus (Bloch). Int J Environ Res Pub Health 7:3298–3312

Onyango M, Matsuda H, Ogada T (2003) Sorption kinetics of arsenic onto iron-conditioned zeolite. J Chem Eng Jpn 36:477–485

Phyu YL, Warne MS, Lim RP (2004) Toxicity of atrazine and molinate to the cladoceran *Daphnia carinata* and the effect of river water and bottom sediment on their bioavailability. Arch Environ Contam Toxicol 46:308–315

Ritter WF (1990) J Environ Sci Health B 25:1–29

Sanagi MM, Muhammad SS, Hussain I, Ibrahim WAW, Ali I (2015) Novel solid-phase membrane tip extraction and gas chromatography with mass spectrometry methods for the rapid analysis of triazine herbicides in real waters. J Sep Sci (in press). doi:10.1002/jssc.201400912

Shahwan T, AbuSirriah S, Nairat M, Boyac E, Eroglu AE, Scott TB, Hallam KR (2011) Green synthesis of iron nanoparticles and their application as a Fenton-like catalyst for the degradation of aqueous cationic and anionic dyes. Chem Eng J 172:258–266

Silva CR, Gomes TF, Andrade GC, Monteiro SH, Dias AC, Zagatto EA, Tornisielo VL (2013) Banana peel as an adsorbent for removing atrazine and ametryne from waters. J Agric Food Chem 61:2358–2363

Southwick LM, Grigg BC, Kornecki TS, Fouss JL (2002) Potential influence of sugarcane cultivation on estuarine water quality of Louisiana's gulf coast. J Agric Food Chem 50:4393–4399

Stevens JT, Sumner DD (1991) Herbicides. In: Hayes WJ Jr, Laws ER Jr (eds) Handbook of pesticide toxicology. Academic Press, New York

Thorpe N, Shirmohammadi A (2005) Herbicides and nitrates in groundwater of Maryland and childhood cancers: a geographic information systems approach. J Environ Sci Health C Environ Carcinog Ecotoxicol Rev 23:261–278

U.S. ATSDR (2003) Toxicological profile for atrazine, 2003. http://www.atsdr.cdc.gov/toxprofiles/tp153.html

U.S. EPA (2003) Atrazine Interim Reregistration Eligibility Decision, 2003. http://www.epa.gov/oppsrrd1/REDs/atrazine_ired.pdf

Van Leeuwen JA, Waltner-Toews D, Abernathy T, Smit B, Shoukri M (1999) Associations between stomach cancer incidence and drinking water contamination with atrazine and nitrate in Ontario (Canada) agroecosystems, 1987–1991. Int J Epidemiol 28:836–840

Villanueva CM, Durand G, Coutte M, Chevrier C, Cordier S (2005) Atrazine in municipal drinking water and risk of low birth weight, preterm delivery, and small-for-gestational-age status. Occup Environ Med 62:400–405

Watson DG (1999) Pharmaceutical analysis: a text book of pharmacy students and pharmaceutical chemists. Wiley, London

Yoder J, Watson M, Benson WW (1973) Lymphocyte chromosome analysis of agricultural workers during extensive occupational exposure to pesticides. Mutilation Res 21:335–340

Yola ML, Eren T, Atar N (2014) A novel efficient photocatalyst based on TiO_2 nanoparticles involved boron enrichment waste for photocatalytic degradation of atrazine. Chem Eng J 250:288–294

Zhang Y, Li Y, Zheng X (2011) Removal of atrazine by nanoscale zero valent iron supported on organobentonite. Sci Total Environ 409:625–630

Zhao X, Ouyang W, Hao F, Lin C, Wang F, Han S, Geng X (2013) Properties comparison of biochars from corn straw with different pretreatment and sorption behaviour of atrazine. Bioresour Technol 147:338–344